Models for Linear Acetylide Polymers: Synthesis and Single-Crystal X-ray Structures of the Ruthenium(II) Acetylide and Diacetylides $Ru(CO)_2(PEt_3)_2[(C{\equiv}C)_nR]_2$ (n = 1, R = Me_3Si; n = 2, R = Me_3Si, H)

Yan Sun, Nicholas J. Taylor, and Arthur J. Carty*

Guelph-Waterloo Center for Graduate Work in Chemistry, Waterloo Campus, Department of Chemistry, University of Waterloo, Waterloo, Ontario N2L 3G1, Canada

Received May 18, 1992

As model compounds for long-chain, linear, acetylide-based polymers, the bis(acetylides) and bis(diacetylides) of ruthenium(II) *trans*-$Ru(CO)_2(PEt_3)_2[(C{\equiv}C)_nR]_2$ (**2**, n = 1, R = Me_3Si; **3**, n = 2, R = Me_3Si; **4**, n = 2, R = H) have been synthesized and fully characterized by IR and Raman spectroscopy, ^1H, $^{13}C\{^1H\}$, and $^{31}P\{^1H\}$ NMR studies, and single-crystal X-ray diffraction. Complex **2** crystallizes in the monoclinic space group $P2_1/c$ with Z = 2 in a unit cell of dimensions a = 11.733 (3) Å, b = 10.944 (3) Å, c = 13.414 (4) Å, and β = 111.65 (2)°. The structure was solved and refined using 4091 observed reflections measured on a Siemens R3m/v diffractometer to a final R value of 2.66%. Crystals of **3** are monoclinic, space group $P2_1/c$, with a = 13.980 (4) Å, b = 10.324 (2) Å, c = 13.146 (3) Å, β = 115.18(2)°, and Z = 2. On the basis of 4141 observed reflections, the structure was refined to R = 2.79%. Crystals of **4** are monoclinic, space group $P2_1/c$, with a = 7.642 (2) Å, b = 9.167 (2) Å, c = 16.493 (3) Å, β = 93.05 (2)°, and Z = 2. For 2905 observed reflections R was 2.56%. All three structure determinations were of high quality. Comparison of bond lengths between these complexes and related acetylides suggests that the trimethylsilyl-substituted bis(acetylides) or bis(diacetylides) have greater multiple-bond character in metal to acetylene σ bonds than other acetylide derivatives.

Introduction

Linear transition-metal σ-acetylide polymers continue to attract considerable attention due to their potential applications in the materials science field.[1] Interest in such molecules stems from (i) evidence that certain long-chain Pt(II), Pd(II) acetylides exhibit liquid crystalline behavior,[1a,e] (ii) the demonstration of nonlinear optical properties for short-chain oligomeric and polymeric acetylides,[2] and (iii) the potential of acetylide monomers, oligomers, and polymers as precursors of metal carbide phases.[3] Our work was stimulated by a longstanding interest in polynuclear acetylides and the observation that relatively few *trans*-bis(σ-acetylides) and *trans*-bis(σ-diacetylides) have been structurally characterized.[2b,4] Thus, until recently the only known Ru(II) bis(acetylides) were the unsymmetrical cis complexes $Ru(CO)_2(C{\equiv}CPh)_2(PPr^i_3)_2$ and the *cis,trans*-$Ru(PMe_3)_2(C{\equiv}CPh)_2(CO)(PPr^i_3)$ compounds prepared by Werner et al.[5a] and a bis(diynyl)ruthenium complex, $(dppm)_2Ru[-C{\equiv}CC{\equiv}CC(OSiMe_3)Ph_2]_2$, by Dixneuf and co-workers.[5b] Similarly, to date the only structurally characterized ruthenium diacetylide is $(\eta^6\text{-}C_6Me_6)(PMe_3)(Cl)Ru{-}C{\equiv}CC{\equiv}CC(OSiMe_3)Ph_2$, a mono(diynyl)ruthenium(II) compound.[6] Although for other transition metals systematic investi-

Scheme I

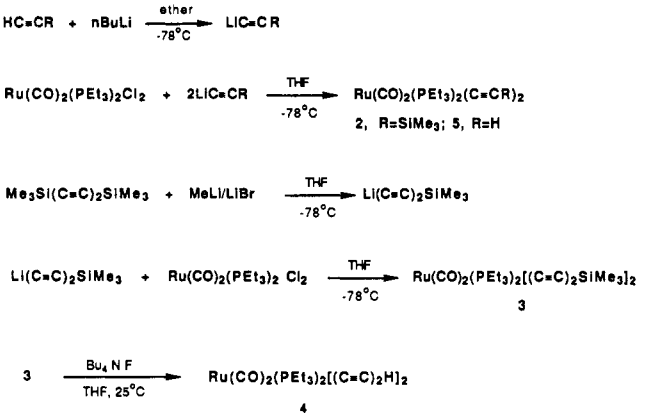

(1) See for example: (a) Hagihara, N.; Sonogashira, K.; Takahashi, S. *Adv. Poly. Sci.* **1981**, *41*, 149. (b) Ogawa, H.; Onitsuka, K.; Joh, T.; Takahashi, S. *Organometallics* **1988**, *7*, 2257. (c) Hanabusa, K.; Higashi, J.; Koyama, T.; Shirai, H.; Hojo, N.; Kurose, A. *Makromol. Chem.* **1989**, *190*, 1. (d) Davies, S. J.; Johnson, B. F. G.; Lewis, J.; Khan, M. S. *J. Organomet. Chem.* **1991**, *401*, C43. (e) Takahashi, S.; Takai, Y.; Morimoto, H.; Sonogashira, K. *J. Chem. Soc., Chem. Commun.* **1984**, 3. (f) Johnson, B. F. G.; Kakkar, A. K.; Khan, M. S.; Lewis, J.; Dray, A. E.; Wittmann, F.; Friend, R. H. *J. Mater. Chem.* **1991**, *1*, 485. (g) Lewis, J.; Khan, M. S.; Kakkar, A. K.; Johnson, B. F. G.; Marder, T. B.; Fyfe, H. B.; Wittmann, F.; Friend, R. H.; Dray, A. E. *J. Organomet. Chem.* **1992**, *425*, 165. (h) Khan, M. S.; Davies, S. J.; Kakkar, A. K.; Schwartz, D.; Lin, B.; Johnson, B. F. G.; Lewis, J. *J. Organomet. Chem.* **1992**, *424*, 87. (i) Davies, S. J.; Johnson, B. F. G.; Lewis, J.; Raithby, P. R. *J. Organomet. Chem.* **1991**, *414*, C51. (j) Johnson, B. F. G.; Kakkar, A. K.; Khan, M. S.; Lewis, J. *J. Organomet. Chem.* **1991**, *409*, C12. (k) Davies, S. J.; Johnson, B. F. G.; Khan, M. S.; Lewis, J. *J. Chem. Soc., Chem. Commun.* **1991**, 187. (l) Khan, M. S.; Pasha, N. A.; Kakkar, A. K.; Raithby, P. R.; Lewis, J.; Wittmann, F.; Fuhrmann, K.; Friend, R. H. *J. Mater. Chem.*, in press. (m) Khan, M. S.; Pasha, N. A.; Kakkar, A. K.; Raithby, P. R.; Lewis, J.; Fuhrmann, K.; Friend, R. H. *J. Mater. Chem.* **1992**, *2*, 759.

(2) (a) Guha, S.; Frazier, C. C.; Kang, K.; Finberg, S. E. *Opt. Lett.* **1989**, *14*, 952. (b) Marder, T. B.; Lesley, G.; Yuan, Z.; Fyfe, H. B.; Chow, P.; Stringer, G.; Jobe, I. R.; Taylor, N. J.; Williams, I. D.; Kurtz, S. K. *Materials for Nonlinear Optics: Chemical Perspectives*; ACS Symposium Series 455; American Chemical Society: Washington, DC, 1991; Chapter 40, p 605. (c) Blau, W. J.; Byrne, H. J.; Cardin, D. J.; Davey, A. P. *J. Mater. Chem.* **1991**, *1*, 245. (d) Frazier, C. C.; Guha, S.; Chen, W. P.; Cockerham, M. P.; Porter, P. L.; Chauchard, E. A.; Lee, C. H. *Polymer* **1987**, *28*, 533.

(3) Wynne, K. J.; Rice, R. W. *Annu. Rev. Mater. Sci.* **1984**, *14*, 297.

(4) (a) Chow, P.; Zargarian, D.; Taylor, N. J.; Marder, T. B. *J. Chem. Soc., Chem. Commun.* **1989**, 1545. (b) Field, L. D.; George, A. V.; Hambley, T. W.; Malouf, E. Y.; Yound, D. J. *J. Chem. Soc., Chem. Commun.* **1990**, 931. (c) Field, L. D.; George, A. V.; Malouf, E. Y.; Slip, I. H. M.; Hambley, T. W. *Organometallics* **1991**, *10*, 3842. (d) Stang, P. J.; Tykwinski, R. *J. Am. Chem. Soc.* **1992**, *114*, 4411. (e) Ramsden, J. A.; Weng, W.; Arif, A. M.; Gladysz, J. A. *J. Am. Chem. Soc.* **1992**, *114*, 5890. (f) Worth, G. H.; Robinson, B. H.; Simpson, J. *Organometallics* **1992**, *11*, 501.

(5) (a) Werner, H.; Meyer, U.; Esteruelas, M. A.; Sola, E.; Oro, L. A. *J. Organomet. Chem.* **1989**, *366*, 187. (b) Pirio, N.; Touchard, D.; Dixneuf, P. H. *Angew. Chem., Int. Ed. Engl.* **1992**, *31*, 651.

(6) Romero, A.; Peron, D.; Dixneuf, P. H. *J. Chem. Soc., Chem. Commun.* **1990**, 1410.

0276-7333/92/2311-4293$03.00/0

gations of acetylide synthesis and reactivity have been carried out,[4] relatively few diacetylides have been characterized and neither their structural chemistry nor reactivity have been explored in detail.[2b] There are for instance no examples of well-characterized σ-butadiynyl (-C≡CC≡CH) complexes. In a recent communication we have briefly outlined a route to symmetrical bis(alkynyl) and bis(dialkynyl) complexes of Ru(II).[7] In this paper we describe in detail a strategy for the synthesis of acetylides and diacetylides with terminal C-H groups. The first single-crystal X-ray analysis of a bis(butadiynyl) complex, *trans*-$Ru(CO)_2(PEt_3)_2(C{\equiv}CC{\equiv}CH)_2$ (**4**), the bis((trimethylsilyl)ethynyl) compound *trans*-$Ru(CO)_2(PEt_3)_2(C{\equiv}CSiMe_3)_2$ (**2**), and the bis((trimethylsilylbutadiynyl) complex *trans*-$Ru(CO)_2(PEt_3)_2(C{\equiv}CC{\equiv}CSiMe_3)_2$ (**3**) are described. An analysis of bonding features within the -C≡C—M—C≡C- and -C≡CC≡C—M—C≡CC≡C- chains of these complexes is presented.

Results and Discussion

Synthesis. The ruthenium(II) carbonyl phosphine complex *trans*-$Ru(CO)_2(PEt_3)_2Cl_2$ (**1**) is readily prepared in high yield from $RuCl_3{\cdot}xH_2O$ via treatment with CO and PEt_3 in ethanol and is a very useful starting material for the synthesis of η^1-hydrocarbyl compounds via treatment with organolithium reagents. Thus, reaction of **1** with 2 equiv of lithium (trimethylsilyl)acetylide, $LiC{\equiv}CSiMe_3$, in THF afforded good yields of $Ru(CO)_2(PEt_3)_2(C{\equiv}CSiMe_3)_2$ (**2**). Following conversion of the bis(trimethylsilyl)diyne $Me_3SiC{\equiv}CC{\equiv}CSiMe_3$ to $Me_3SiC{\equiv}CC{\equiv}CLi$ via treatment with MeLi/LiBr, reaction with **1** gave the bis(diacetylide) complex $Ru(CO)_2(PEt_3)_2(C{\equiv}CC{\equiv}CSiMe_3)_2$ (**3**) in good yield. The transformation of the TMS-substituted acetylide **3** to the terminal acetylide $Ru(CO)_2(PEt_3)_2(C{\equiv}CC{\equiv}CH)_2$ (**4**) proved to be relatively easy and essentially quantitative, but the isolation of pure, crystalline **3** and particularly **4** was difficult. Protonation of **2** with Bu_4NF in THF failed, and the parent acetylide compound $Ru(CO)_2(PEt_3)_2(C{\equiv}CH)_2$ (**5**) was obtained from the reaction of **1** with HC≡CLi directly, with HC≡CLi being prepared from gaseous HC≡CH and ^{n}BuLi in situ (Scheme I). Complexes **3**–**5** are susceptible to oligomerization and are sensitive to air, light, and moisture, necessitating extreme care and attention during isolation. Crystals of **3**–**5** for X-ray analysis were obtained from highly concentrated solutions, following several sequences of purification.

Spectroscopy. The identities of complexes **2**–**5** were based on their FTIR and ^1H, $^{13}C\{^1H\}$, ^{13}C, and $^{31}P\{^1H\}$ NMR spectra.[7] All all-trans configuration of these compounds was clearly shown by the simple singlet pattern of their ν(CO) IR and ^{31}P NMR spectra. In the case of the bis(diacetylides), two bands due to ν(C≡C) of the diacetylides, corresponding to the free and coordinated alkynyl moieties, were observed. The ^{13}C NMR spectra of compounds **2**–**5** were assigned on the basis of ^{13}C–^{31}P and ^{13}C–^1H coupling constants and ^{13}C chemical shifts. Thus, for **2** a downfield triplet resonance at δ 198.1 ppm with $^2J_{P-C}$ = 13.4 Hz is attributed to the two CO groups cis to the PEt_3 ligands. The α-carbon resonance is also a triplet from coupling to two equivalent ^{31}P nuclei (δ 128.4 ppm, J = 12.4 Hz), and the β-carbon atom of the acetylides appears as a singlet with a low-field chemical shift (δ 116.1 ppm). A similar downfield shift has been reported for a bis(trimethylsilyl)alkynyl-substituted cyclobutenedione and explained by hyperconjugative resonance contributions.[8a] The ethynyl and butadiynyl complexes **5** and **4** have several interesting NMR features. For **5** C_α gives rise to a triplet resonance at 98.5 ppm ($^2J_{P-C}$ = 13.0 Hz), while C_β is a singlet in the $^{13}C\{^1H\}$ spectrum and a doublet at 95.0 ppm ($^1J_{C-H}$ = 222.9 Hz) in the proton-coupled spectrum. The terminal proton resonance in **5** is a triplet due to long-range coupling ($^4J_{P-H}$ = 1.69 Hz) to phosphorus. In **4** there is a remarkable six-bond coupling ($^6J_{P-H}$) to the acetylenic hydrogen nucleus ($^6J_{P-H}$ = 0.8 Hz), a fact which suggests that there must be electronic communication from phosphorus through the metal atoms and along the -C≡CC≡C- chain. The ^{13}C resonances of C(2) to C(5) follow from comparisons with **5**, **2**, and **3**, with chemical shifts falling in the sequence (ppm) C(2) > C(3) > C(4) > C(5), with C(5) being at highest field (C(2) is bound to Ru). There are very few ^{13}C data for bis(diacetylides) such as **4** and **5** in the literature for comparison.[8b]

In compounds **2**–**5** the ν(CO) infrared frequencies lie in the range 1986–2002 cm^{-1}, values which compare with a ν(CO) value of 1993 cm^{-1} in the Ru(II) precursor **1**. These frequencies presumably reflect the relative electron-withdrawing capabilities of -Cl vs -C≡CR as well as competition between -CO and -C≡CR for metal dπ electrons. The ν(C≡C) value for the parent acetylide **5** (1944 cm^{-1}) is much lower than those for other related bis(acetylides) (2021 cm^{-1} for *trans*-$Ru(CO)_2(PEt_3)_2(C{\equiv}CSiMe_3)_2$ (**2**) and 2093 cm^{-1} for the phenyl derivative *trans*-$Ru(CO)_2(PEt_3)_2(C{\equiv}CPh)_2$ (**7**)[7]). The fact that monosubstituted (HC≡CR) acetylenes have lower ν(C≡C) frequencies than their RC≡CR′ counterparts (by 100–150 cm^{-1}) is well established.[9] As a consequence it is not possible to correlate changes in ν(C≡C) for terminal and substituted acetylides with changes in -C≡C- bond strength. The lowering in frequency of the trimethylsilyl-substituted acetylide **2** relative to that of hydrocarbyl derivative **7** may suggest a weakening of the triple bond in molecule **2**. In fairly symmetrical molecules such as these acetylides, some of the vibrations do not cause a significant change in dipole moment essential for infrared absorption. Therefore, we also carried out a Raman study on the two acetylides (symmetric C≡C stretching frequencies: **2**, ν′(C≡C) 2030 cm^{-1}; **7**, ν′(C≡C) 2109 cm^{-1}) to confirm the assignment. If we take the average of ν and ν′ for each molecule (**2**, 2026 cm^{-1}; **7**, 2101 cm^{-1}), the same conclusion, namely that the triple bond in **2** is weaker than in **7**, can be reached.

The two peaks (2165 and 2121 cm^{-1}) of the diacetylide **3** in the acetylenic region of the FTIR spectrum were assigned on the basis of their bond lengths. Thus, the band at lower energy (2121 cm^{-1}) is more likely due to the -C≡C- triple bond adjacent to the metal center, since this bond has the longer bond length (1.226 (2) vs. 1.209 (2) Å; Figure 4). In the bis(butadiynyl) complex **4**, only one peak is observed at 2137 cm^{-1}. This absorption was assigned to the coordinated acetylide vibration, since the other terminal triple bond, C≡CH, is expected to vibrate at lower frequency for the reasons mentioned above and may thus be obscured by the ν(CO) band at ~2000 cm^{-1}. Such an assignment of ν(C≡C) for the Ru σ-bonded acetylides in the two bis(diacetylides) (2121 cm^{-1} for **3**; 2137 cm^{-1} for **4**) also implies that the introduction of terminal alkylsilyl groups on the metal-containing acetylene chain weakens the triple bonds.

(7) Sun, Y.; Taylor, N. J.; Carty, A. J. *J. Organomet. Chem.* **1992**, *423*, C43.

(8) (a) Rubin, Y.; Knobler, C. B.; Diederich, F. *J. Am. Chem. Soc.* **1990**, *112*, 1607. (b) Wong, A.; Kang, P. C. W.; Tagge, C. D.; Leon, D. R. *Organometallics* **1990**, *9*, 1992.

(9) Lambert, J. B.; Shurvell, H. F.; Lightnen, D.; Cooks, R. G. *Introduction to Organic Spectroscopy*; Macmillan: New York, 1987; p 204.

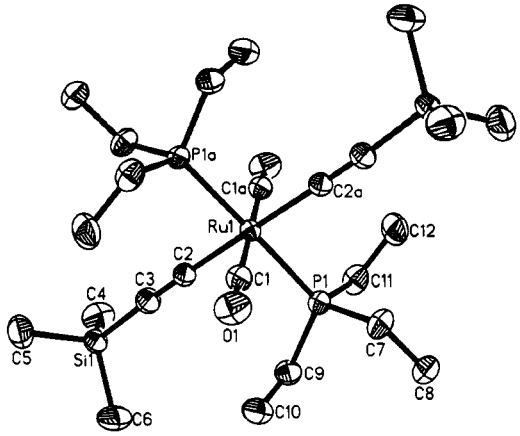

Figure 1. Molecular structure of $Ru(CO)_2(PEt_3)_2(C{\equiv}CSiMe_3)_2$ (**2**). Hydrogen atoms have been omitted for clarity.

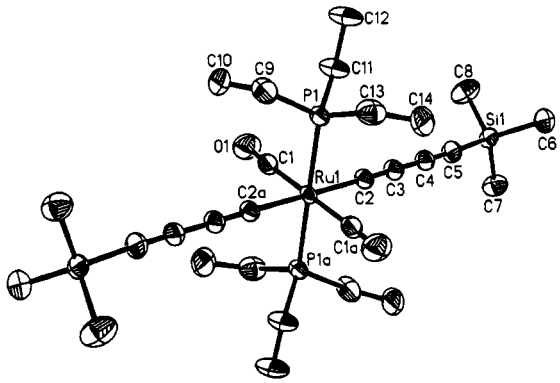

Figure 2. Molecular structure of $Ru(CO)_2(PEt_3)_2(C{\equiv}CC{\equiv}CSiMe_3)_2$ (**3**). Hydrogen atoms have been omitted for clarity.

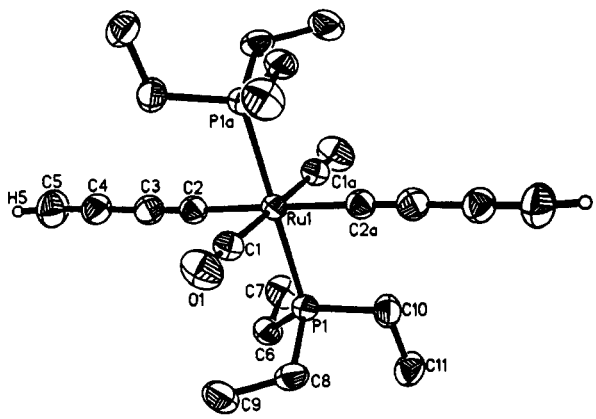

Figure 3. Molecular structure of $Ru(CO)_2(PEt_3)_2(C{\equiv}CC{\equiv}CH)_2$ (**4**). Hydrogen atoms, except for $-C{\equiv}CH$, have been omitted for clarity.

X-ray Structures of 2–4. The structural characterization of compound **5** has been briefly described in a previous communication.[7] The molecular structures of complexes **2–4** are shown in Figures 1–3, respectively. The interatomic parameters for the three compounds are collected in Tables I–III. The crystal structures consist of discrete molecules, with no significant intermolecular interactions. The ruthenium atoms in all cases sit on crystallographic inversion centers in the crystals (see also the packing diagrams for **2** in Figures 5 and 6) and are octahedrally coordinated by two carbonyl groups, two triethylphosphine ligands, and two acetylides in an all-trans pattern. One of the interesting features of these structures is that there is very little distortion from linearity of the

Table I. Bond Lengths (Å) and Angles (deg) for 2

Ru(1)–P(1)	2.369 (1)	Ru(1)–C(1)	1.933 (2)
Ru(1)–C(2)	2.062 (2)	P(1)–C(7)	1.827 (2)
P(1)–C(9)	1.825 (2)	P(1)–C(11)	1.825 (2)
Si(1)–C(3)	1.812 (2)	Si(1)–C(4)	1.868 (2)
Si(1)–C(5)	1.866 (2)	Si(1)–C(6)	1.873 (2)
O(1)–C(1)	1.133 (2)	C(2)–C(3)	1.221 (2)
C(7)–C(8)	1.531 (2)	C(9)–C(10)	1.529 (3)
C(11)–C(12)	1.517 (3)		
P(1)–Ru(1)–C(1)	89.1 (1)	P(1)–Ru(1)–C(2)	90.1 (1)
C(1)–Ru(1)–C(2)	92.7 (1)	P(1)–Ru(1)–P(1A)	180.0 (1)
P(1)–Ru(1)–C(1A)	90.9 (1)	C(1)–Ru(1)–C(1A)	180.0 (1)
P(1)–Ru(1)–C(2A)	89.9 (1)	C(1)–Ru(1)–C(2A)	87.3 (1)
C(2)–Ru(1)–C(2A)	180.0 (1)	Ru(1)–P(1)–C(7)	113.9 (1)
Ru(1)–P(1)–C(9)	116.1 (1)	C(7)–P(1)–C(9)	104.8 (1)
Ru(1)–P(1)–C(11)	114.6 (1)	C(7)–P(1)–C(11)	104.6 (1)
C(9)–P(1)–C(11)	101.3 (1)	C(3)–Si(1)–C(4)	109.8 (1)
C(3)–Si(1)–C(5)	110.0 (1)	C(4)–Si(1)–C(5)	110.0 (1)
C(3)–Si(1)–C(6)	109.2 (1)	C(4)–Si(1)–C(6)	109.0 (1)
C(5)–Si(1)–C(6)	108.9 (1)	Ru(1)–C(1)–O(1)	178.0 (1)
Ru(1)–C(2)–C(3)	178.1 (1)	Si(1)–C(3)–C(2)	176.1 (1)
P(1)–C(7)–C(8)	116.6 (1)	P(1)–C(9)–C(10)	114.5 (1)
P(1)–C(11)–C(12)	114.4 (2)		

Table II. Bond Lengths (Å) and Angles (deg) for 3

Ru(1)–P(1)	2.373 (1)	Ru(1)–C(1)	1.935 (2)
Ru(1)–C(2)	2.057 (2)	P(1)–C(9)	1.814 (2)
P(1)–C(11)	1.814 (2)	P(1)–C(13)	1.825 (2)
Si(1)–C(5)	1.831 (2)	Si(1)–C(6)	1.868 (3)
Si(1)–C(7)	1.863 (3)	Si(1)–C(8)	1.854 (3)
O(1)–C(1)	1.131 (3)	C(2)–C(3)	1.226 (2)
C(3)–C(4)	1.370 (2)	C(4)–C(5)	1.209 (2)
C(9)–C(10)	1.538 (6)	C(11)–C(12)	1.537 (4)
C(13)–C(14)	1.509 (4)		
P(1)–Ru(1)–C(1)	89.2 (1)	P(1)–Ru(1)–C(2)	89.8 (1)
C(1)–Ru(1)–C(2)	86.9 (1)	P(1)–Ru(1)–P(1A)	180.0 (1)
P(1)–Ru(1)–C(1A)	90.8 (1)	C(1)–Ru(1)–C(1A)	180.0 (1)
P(1)–Ru(1)–C(2A)	90.2 (1)	C(1)–Ru(1)–C(2A)	93.1 (1)
C(2)–Ru(1)–C(2A)	180.0 (1)	Ru(1)–P(1)–C(9)	116.1 (1)
Ru(1)–P(1)–C(11)	114.0 (1)	C(9)–P(1)–C(11)	104.8 (1)
Ru(1)–P(1)–C(13)	114.6 (1)	C(9)–P(1)–C(13)	101.6 (1)
C(11)–P(1)–C(13)	104.3 (1)	C(5)–Si(1)–C(6)	108.8 (1)
C(5)–Si(1)–C(7)	109.3 (1)	C(6)–Si(1)–C(7)	110.1 (1)
C(5)–Si(1)–C(8)	108.3 (1)	C(6)–Si(1)–C(8)	108.2 (1)
C(7)–Si(1)–C(8)	112.0 (1)	Ru(1)–C(1)–O(1)	177.3 (2)
Ru(1)–C(2)–C(3)	176.5 (2)	C(2)–C(3)–C(4)	178.9 (2)
C(3)–C(4)–C(5)	179.8 (3)	Si(1)–C(5)–C(4)	177.2 (2)
P(1)–C(9)–C(10)	114.6 (2)	P(1)–C(11)–C(12)	115.9 (2)
P(1)–C(13)–C(14)	114.0 (2)		

Table III. Bond Lengths (Å) and Angles (deg) for 4

Ru(1)–P(1)	2.381 (1)	Ru(1)–C(1)	1.943 (2)
Ru(1)–C(2)	2.078 (2)	P(1)–C(6)	1.829 (2)
P(1)–C(8)	1.829 (2)	P(1)–C(10)	1.831 (2)
O(1)–C(1)	1.125 (2)	C(2)–C(3)	1.194 (2)
C(3)–C(4)	1.386 (3)	C(4)–C(5)	1.196 (3)
C(6)–C(7)	1.525 (3)	C(8)–C(9)	1.533 (3)
C(10)–C(11)	1.525 (2)		
P(1)–Ru(1)–C(1)	91.6 (1)	P(1)–Ru(1)–C(2)	92.0 (1)
C(1)–Ru(1)–C(2)	92.1 (1)	P(1)–Ru(1)–P(1A)	180.0 (1)
P(1)–Ru(1)–C(1A)	88.4 (1)	C(1)–Ru(1)–C(1A)	180.0 (1)
P(1)–Ru(1)–C(2A)	88.0 (1)	C(1)–Ru(1)–C(2A)	87.9 (1)
C(2)–Ru(1)–C(2A)	180.0 (1)	Ru(1)–P(1)–C(6)	117.0 (1)
Ru(1)–P(1)–C(8)	113.3 (1)	C(6)–P(1)–C(8)	103.2 (1)
Ru(1)–P(1)–C(10)	112.5 (1)	C(6)–P(1)–C(10)	104.8 (1)
C(8)–P(1)–C(10)	104.7 (1)	Ru(1)–C(1)–O(1)	177.8 (2)
Ru(1)–C(2)–C(3)	177.9 (1)	C(2)–C(3)–C(4)	176.9 (2)
C(3)–C(4)–C(5)	178.9 (2)	P(1)–C(6)–C(7)	113.9 (1)
P(1)–C(8)–C(9)	112.8 (1)	P(1)–C(10)–C(11)	116.5 (1)

$-C{\equiv}C-Ru-C{\equiv}C-$ and $-C{\equiv}CC{\equiv}C-Ru-C{\equiv}CC{\equiv}C-$ chains. For example, the Ru(1)–C(2)–C(3) angle in molecule **3** is 176.5 (2)°, and this is the largest deviation from linearity in any of the three structures. These small deviations from linearity are probably due to crystal-packing

forces, since acetylenes are known to be relatively soft ligands.[10]

The bond distances between carbon atoms in the linear chains of **2–4** show bond length alternations, as found in other related acetylides.[2b,4,11] Carbon–carbon triple-bond lengths are relatively insensitive to electronic changes, and –C≡C– distances usually vary little from the values in free actylenes (~1.20 Å). In compounds such as these transition-metal acetylides the extent of π back-bonding between metals and acetylenic ligands is still a matter of debate in the literature. Generally speaking, structural evidence for π back-bonding relies heavily on the shortening of M—C bonds and the corresponding C≡C bond elongations. In practice, however, the relatively small difference between C≡C bond lengths in transition-metal acetylides and those in free acetylenes essentially limits meaningful comparisons of structural differences to molecules whose structures have been determined with great precision. Fortunately, in the present cases the high X-ray diffraction quality of the single crystals of **2–4** combined with low-temperature data collection and intensity measurements out to high 2θ angles (4–60°) allowed the acquisition of very accurate data sets. Thus, a systematic comparison of structural changes for a series of acetylides having the same basic geometry, the same central metal atom, and ancillary ligands was possible.

The only chemical difference between compounds **3** and **4** is the substituent group R on the acetylides (Figure 4). The presence of a trimethylsilyl group at the end of a metal-containing acetylene chain as in **3** causes a shortening of the formally single bonds in **3** vs **4** (Ru–C(2), 2.057 (2) vs 2.078 (2) Å; C(3)–C(4), 1.370 (2) vs 1.386 (3) Å) and a lengthening of the triple bonds (C(2)–C(3), 1.226 (2) vs 1.194 (2) Å; C(4)–C(5), 1.209 (2) vs 1.196 (3) Å. A similar trend is evident in the changes in bond lengths which occur upon substituting the H atoms in the parent acetylide **5** with $SiMe_3$ groups in **2**. Thus, the formal single bond between Ru and C_α is shortened (2.062 (2) Å in **2** vs 2.078 (1) Å in **5**), and the triple bond is elongated (1.221 (2) Å in **2** vs 1.199 (2) Å in **5**). In fact, the bond length of the C≡C triple bond adjacent to Ru (2.226 (2) Å) in compound **3** is one of the longest distances yet reported for an acetylide complex. In the structure of the related molecule $(\eta^6\text{-}C_6Me_6)(PMe_3)(Cl)Ru{-}C{\equiv}CC{\equiv}CC(OSiMe_3)Ph_2$[6] recently described, a longer C≡C distance of 1.26 (4) Å has been reported. Unfortunately, however, the latter determination is of relatively low precision and the estimated standard deviations on carbon–carbon bond lengths do not permit a realistic comparison with **2** or **3**. The apparent lengthening of the C≡C bonds in **2** and **3** may suggest a greater contribution to metal–carbon multiple bonding from Ru(dπ)–C(pπ^*) back-bonding than in acetylides not bearing Me_3Si substituents. The presence and importance of M–C(carbonyl) dπ–pπ^* back-bonding in metal carbonyl complexes is generally accepted, being manifest in the lowering of ν(C≡O) frequencies of carbonyl ligands compared to the value of ν(C≡O) in free carbon monoxide. In fact, ν(C≡O) in metal carbonyls is a relatively sensitive measure of electron transfer from CO ligands via the metal center to CO π^* orbitals.[12] In contrast, C≡O bond lengths in carbonyl complexes are much less sensitive to changes in π-bonding, and the range of values in complexes **2–5** (1.125 (2)–1.133 (1) Å) differs little from the bond length in free CO (1.128 Å).[12] For the acetylides, however, there is a good correlation between the ν(C≡C) stretching frequencies and the corresponding triple-bond lengths with the lower ν(C≡C) values in the $SiMe_3$-substituted compounds **2** and **3** correlating with longer bonds. These observations reinforce our conclusion that back-bonding to the acetylide is greater in the $SiMe_3$-substituted complexes. We believe that the changes in Ru—C and C≡C bond lengths observed in the structures of **2–4** are significant and that the shortening of Ru—C and lengthening of C≡C bond distances are evidence for greater delocalization along the $RuC{\equiv}CSiMe_3$ and $RuC{\equiv}CC{\equiv}CSiMe_3$ chains in Me_3Si-substituted compounds. This conclusion is consistent with other physical evidence for electron transfer. Thus, it has been reported that the introduction of R_3Si groups at the ends of polyyne chains results in red shifts in electronic spectra.[13] a fact which has been attributed to Si dπ–polyyne pπ interactions.[11b] In the case of **2** and **3** the metal center provides an additional reservoir for delocalization.

Recently, structural evidence for the first (alkenylallenylidene)ruthenium complex, $(NP_3)Ru(Cl){=}C(1){=}C(2){=}C(3)(OMe)CH{=}CPh_2$ ($NP_3 = N(CH_2CH_2PPh_2)_3$), has been presented.[14] The Ru–C(1), C(1)–C(2), and C(2)–C(3) bond distances in this molecule were reported to be 1.921 (5), 1.254 (7), and 1.369 (7) Å, respectively, as shown in Figure 4. This molecule might alternatively be described as a cationic acetylide (Figure 4) with an unsaturated ligand system in which the carbene-like substituent –C(OMe)CH=CPh_2 bears an electron-donor OMe group. The C(1)–C(2) distance of 1.254 (7) Å in the latter complex compares with the C(2)–C(3) bond length of 1.226 (2) Å in **3** and the standard C≡C distance of 1.20 Å in HC≡CH. Bearing in mind the four-electron-donor ligands in the above cumulene complex $(NP_3)Ru(Cl){=}C{=}C{=}C(OMe)CH{=}CPh_2$ compared to two CO groups and two PEt_3 ligands in **3**, the lengthening of the C≡C bond in **3** appears significant. In support of these arguments the bond lengths in complex **4**, having no $SiMe_3$ substituents, show no unusual features. Other transition-metal acetylides bearing hydrocarbyl substituents with no π-acceptor capabilities are also unremarkable in terms of M—C and C≡C bond lengths.[2b,4]

Additional evidence in support of the conclusion that the C≡C and Ru—C bond lengths indicate delocalization along the $RuC{\equiv}CSi$ and $RuC{\equiv}CC{\equiv}CSi$ chains comes from an analysis of the Ru—C(acetylene) and C—C single-bond distances in **2–5**. Although the metal–acetylide (Ru–C(2)) bond lengths in **2** and **3** are not as short as that in the proposed ruthenium allenylidene complex **6**, the formally single bond C(3)–C(4) (1.370 (2) Å) in **3** is very comparable to the corresponding distance (C(2)–C(3) = 1.369 (7) Å) in **6**, which is presumed to have double-bond character. In sharp contrast the C(3)–C(4) distance in **4** (1.386 (2) Å) is significantly longer, at the 3σ level, than in **3**.

Polyalkynylsilanes, $-[C{\equiv}CSiR_1R_2C{\equiv}CZ]-$, where Z stands for an aromatic group, have been synthesized.[15] These polymers, containing acetylene and aromatic units along with alkylsilyl groups, exhibit electrically semicon-

(10) Torkington, P. *Proc. F. Soc. London* **1951**, *A206*, 17.

(11) See, for example: (a) Beddoes, R. L.; Bitcon, C.; Whiteley, M. W. *J. Organomet. Chem.* **1991**, *402*, 85. (b) Coles, B. F.; Hitchcock, P. B.; Walton, D. R. M. *J. Chem. Soc., Dalton Trans.* **1975**, 442. (c) Rubin, Y.; Lin, S. S.; Knobler, C. B.; Anthony, J.; Boldi, A. M.; Diederich, F. *J. Am. Chem. Soc.* **1991**, *113*, 6943.

(12) Cotton, F. A.; Wilkinson, G. *Advanced Inorganic Chemistry*, 4th ed.; Wiley-Interscience: New York, 1988; p 60.

(13) Eastmond, R.; Johnson, T. R.; Walton, D. R. M. *Tetrahedron* **1972**, *28*, 4601.

(14) Wolinska, A.; Touchard, D.; Dixneuf, P. H.; Romero, A. *J. Organomet. Chem.* **1991**, *420*, 217.

(15) (a) Corriu, R. J. P.; Douglas, W. E.; Yang, Z. *J. Polym. Sci., Polym. Lett. Ed.* **1990**, *28*, 431. (b) Corriu, R. J. P.; Gerbier, P.; Guerin, C.; Henner, B. J. L.; Jean, A.; Mutin, P. H. *Organometallics* **1992**, *11*, 2057.

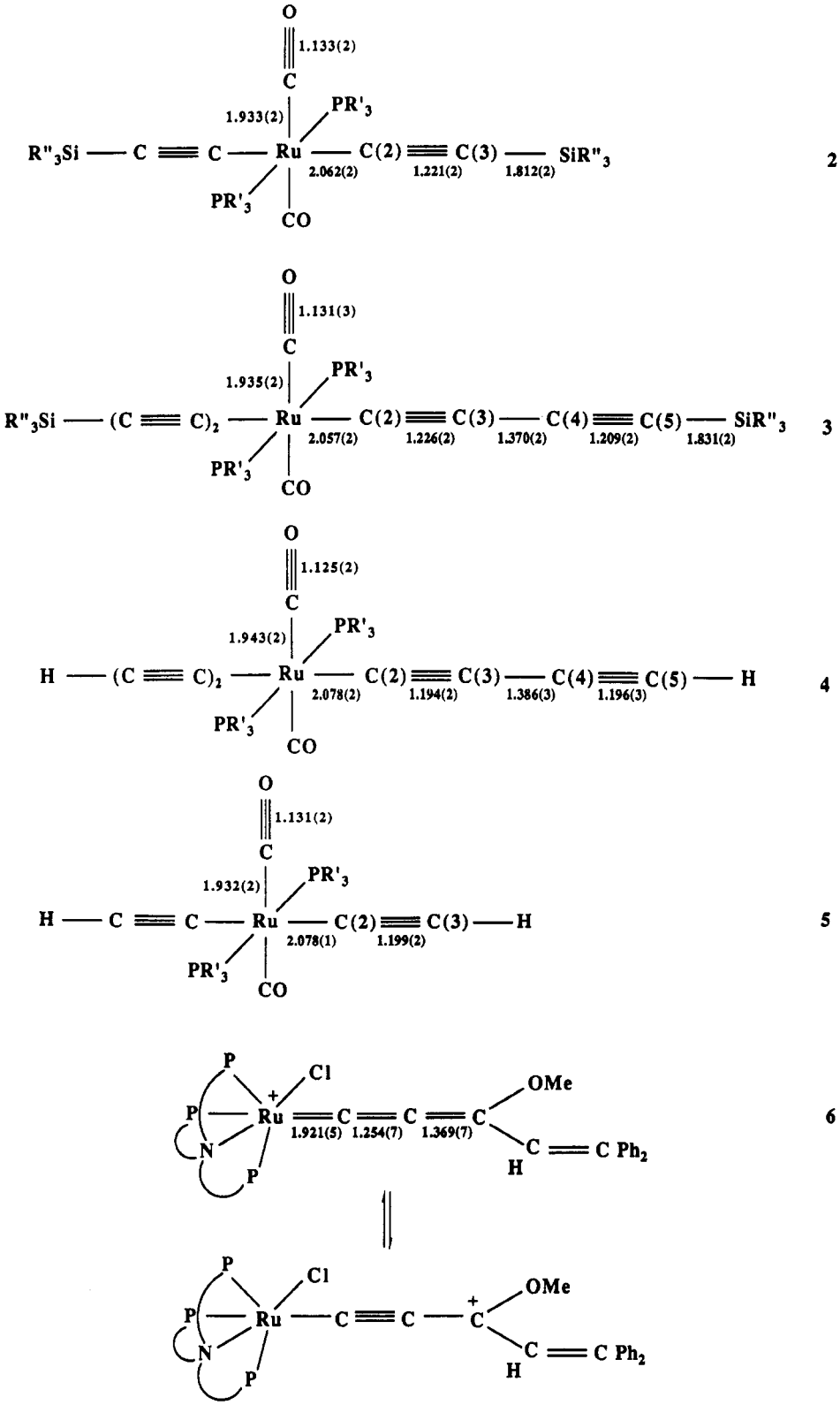

Figure 4. Molecular schemes of **2–4** (this work), **5**,[7] and **6**[14] with selected bond lengths, where R′ = Et and R″ = Me.

ducting properties upon doping with $FeCl_3$.[16] This property is one of the physical characteristics of long-chain conjugated organic polymers and, therefore, suggests the possibility of long-range conjugation in polymer chains containing silicon moieties. This observation adds further support to our proposal that alkylsilyl groups may facilitate electron delocalization along metal-containing polyyne chains by either $d\pi(Si)$–$p\pi(C_{sp})$–$d\pi(M)$ conjugation or $\sigma(Si–C_{sp})$–$p\pi(C_{sp})$–$d\pi(M)$ hyperconjugation.[17]

Although the elongation of –C≡C– and shortening of ≡C—C≡ bonds suggest that electron delocalization from metal to acetylide is greater in a silicon-substituted acetylide, the extent of such conjugation cannot be large, as

(16) Corriu, R. J. P.; Douglas, W. E.; Yang, Y.; Garnier, F.; Yassar, A. *J. Organomet. Chem.* **1991**, *417*, C50.

(17) Pitt, C. G. *J. Organomet. Chem.* **1973**, *61*, 49.

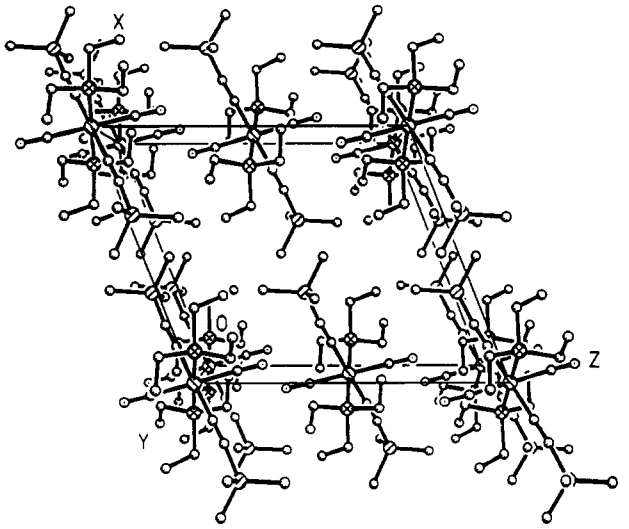

Figure 5. Packing diagram for **2** viewed down the y axis.

can be seen from a comparison of Ru—C(acetylide) (Ru–C(2) = 2.057 (2) Å) with Ru—C(carbonyl) (1.935 (2) Å in **3**) and Ru—C(allenylidene) (1.921 (5) Å in **6**) bond lengths (Figure 4).

It is of interest to compare the two terminal C≡C bond lengths and the differences between the internal C≡C distances in molecules **3** and **4**, since the only difference between these two compounds is in the terminal substituents on the acetylide ligands. In fact, the largest disparity in bond lengths occurs in the center of the chain, that is, between the pair of carbon–carbon triple bonds (with distances of 1.226 (2) Å in **3** and 1.194 (2) Å in **4**; Δ = 0.032 Å) furthest away from the terminal groups. The difference in bond lengths for the other pair of triple bonds adjacent to the terminal substituent is only 0.013 Å. A similar bond length distribution has been reported in $Me_3Si(C{\equiv}C)_4SiMe_3$,[11b] where the central single bond shows the largest reduction from the value expected for a single bond between two sp-hybridized carbon atoms.

The two (alkylsilyl)acetylide derivatives **2** and **3** have very similar structural parameters. The triple bonds are elongated upon substitution of hydrogen by the silicon group, and the bond lengths associated with the carbonyls and phosphines remain almost identical in these two compounds. The largest difference between **2** and **3** is exhibited by the Si–C(C_{sp}) bonds, with the C(5)–Si distance in compound **3** being slightly longer (0.019 Å) than that in **2**, suggesting that the bonding between Si and the C_{sp} carbon atom is stronger in **2** than in **3**. Experimentally, we have observed that **2** and **3** exhibit different behavior toward hydrolytic cleavage with the Bu_4NF reagent, C–$SiMe_3$ cleavage being completed within 30 min for the diacetylide **3** while **2** showed no significant hydrolysis under the same conditions over 24 h.

The packing of the molecules **2**–**4** in the crystal lattices (Figure 5, complex **2**) is interesting, being characterized by two sets of parallel alignments of the acetylide units throughout the unit cells. As required by the glide symmetry of these crystal systems, the two sets are actually oriented differently, forming so-called herringbone patterns which are shown more clearly in the packing diagram projected on the x–y plane (Figure 6, complex **2**). In this diagram, Ru(1c) and Ru(1d) lie above the other two metal atoms, Ru(1a) and Ru(1b) (by $^1/_2c$, where c = 13.414 (4) Å), and the glide planes separate differently oriented molecules. A similar packing arrangement has been reported for two other compounds, *trans*-$Pt(PMe_2Ph)_2(C{\equiv}CC{\equiv}CPh)_2$ (space group $P2_1/c$)[2b] and *trans*-$Ru(CO)_2$-

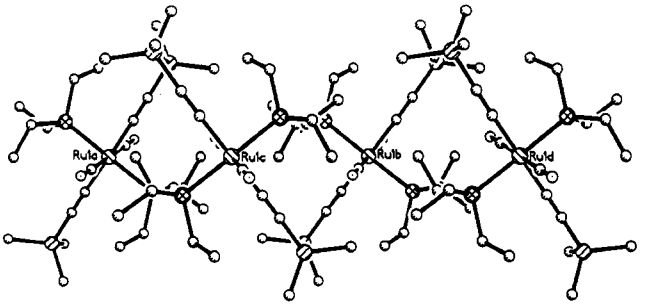

Figure 6. Packing diagram for **2** projected on the x–y plane.

$(PEt_3)_2(C{\equiv}CH)_2$ (space group $P2_1/n$).[7] This form of crystal packing may well be a general feature of transition-metal *trans*-bis(σ-acetylide) complexes bearing glide symmetry. Since the metal centers are octahedrally coordinated Ru(II), the acetylide moieties are well separated from one another in different molecules and, therefore, topochemical polymerization is not possible. Thus, the nearest contact (2.889 Å) in the structure of **4** is between a carbonyl oxygen atom in one molecule and an ethyl group hydrogen (CH_2) atom of a phosphine in a neighboring molecule. In fact, these acetylides appear to be relatively stable once crystallized.

In conclusion, we have characterized three new Ru(II) bis(σ-acetylide) and bis(σ-diacetylides). The extent of electron delocalization along the array of (–C≡C—M—C≡C–) is increased via the introduction of terminal alkylsilyl groups on the chain. Further studies are underway to examine in more detail the role of SiR_3 units in promoting bond conjugation by means of molecular orbital calculations. Our results also suggest that one-dimensional acetylide polyynes with ruthenium(II) centers and –SiR_2– linking units may have interesting electronic properties.

Experimental Section

General Procedures, Chemicals, and Measurements. All synthetic transformations and handling of the compounds were performed under a nitrogen atmosphere in dry, oxygen-free solvents. Silica gel (230–400 mesh) for column chromatography was dried in an oven overnight and cooled under N_2 before use. Thin-layer chromatography (TLC) was carried out on glass plates (20 × 20 cm^2) coated with silica gel (500 μm, Analtech). Infrared spectra were taken in matched 0.5-mm NaCl cells in methylene chloride using a Nicolet 520 FTIR spectrometer. NMR spectra were measured on Bruker AC 200 (or AM 250) spectrometers at 200 or 250 MHz for ^1H, 50.3 or 62.8 MHz for $^{13}C\{^1H\}$ and ^{13}C, and 81.0 or 101.3 MHz for the ^{31}P nucleus, respectively. Shifts are reported with respect to Me_4Si (^1H, ^{13}C) or 85% external H_3PO_4 (^{31}P). Raman spectroscopic data were obtained on a Dilor OMARS-89 spectrometer with a 512-channel diode array optical multichannel analyzer and microscope accessory, interfaced to an IBM PC-AT computer. As excitation light sources, the 514.5-nm line of the Coherent Innova 70 argon ion laser was used. The laser power at the sample was 100 mW. Spectra were recorded by using a 1.25-cm^{-1} band-pass and 1-s photon counting period.

Starting Materials. $Ru(CO)_2(PEt_3)_2Cl_2$ (**1**) was prepared by literature methods[18] and recrystallized from heptane. $HC{\equiv}CSiMe_3$ (Farchan), $SiMe_3C{\equiv}CSiMe_3$ (Aldrich), $SiMe_3C{\equiv}CC{\equiv}CSiMe_3$ (Petrarch Systems Inc.), Bu_4NF (0.1 M solution in THF, Aldrich), MeLi (as a complex with LiBr, 1.2 M solution in diethyl ether, Aldrich), and Bu^nLi (1.6 M solution in hexane, Aldrich) were used as received.

Synthesis. *trans*-$Ru(CO)_2(PEt_3)_2(C{\equiv}CSiMe_3)_2$ (2). The alkyne (0.478 mL) in 10 mL of diethyl ether was cooled to 195 K before the addition of Bu^nLi (2.21 mL). The mixture was stirred at 195 K for 2 h and then transformed via a syringe to a cold (195

(18) Chatt, J.; Shaw, B. L.; Field, A. E. *J. Chem. Soc.* **1964**, 3466.

Table IV. Structure Determination Summaries for 2–4

compd	**2**	**3**	**4**
color, habit	colorless, prism fragment	light golden brown, prism	light-brown prism
cryst size (mm)	0.56 (100) × 0.56 (011) × 0.44 (0$\bar{1}$1)	0.48 (001) × 0.46 (110) × 0.50 (1$\bar{1}$0)	0.22 (100) × 0.27 (001) × (011) × 0.41 (01$\bar{1}$)
cryst syst	monoclinic	monoclinic	monoclinic
space group	$P2_1/c$	$P2_1/c$	$P2_1/c$
unit cell dimens			
a (Å)	11.733 (3)	13.980 (4)	7.642 (2)
b (Å)	10.944 (3)	10.324 (2)	9.167 (2)
c (Å)	13.414 (4)	13.146 (3)	16.497 (3)
β (deg)	111.65 (2)	115.18 (2)	93.05 (2)
V (Å^3)	1601.0 (6)	1716.9 (7)	1154.1 (4)
Z	2	2	2
density (calcd) (g/cm^3)	1.219	1.230	1.414
abs coeff (cm^{-1})	6.68	6.28	8.16
F(000)	620	668	508
diffractometer used		Siemens R3m/v	
radiation		Mo Kα (λ = 0.71073 Å)	
temperature (K)		200	
2θ range (deg)		4.0–60.0	
scan type		ω	
scan speed in ω (deg/min)		variable; 2.93–29.30	
scan range (ω), (deg)		1.20	
std rflns		2 measd every 100 rflns	
abs cor		face-indexed numerical	
no. of rflns collected	4701	5489	3595
no. of indep rflns	4701	5050 (R_{int} = 2.83%)	3378 (R_{int} = 2.84%)
no. of obsd rflns ($F > 6.0\sigma(F)$)	4091	4141	2905
min/max transmissn	0.6744/0.7726	0.7329/0.7945	0.8078/0.8484
system used		Siemens SHELXTL PLUS	
soln		Patterson and Fourier	
refinement method		full-matrix least-squares	
quantity minimized		$\sum w(F_o - F_c)^2$	
H atoms		riding model, refined isotropic U	
extinction cor[a]	yes	no	yes
χ	0.0021 (2)		0.0017 (2)
weighting scheme	$w^{-1} = \sigma^2(F) + 0.0018F^2$	$w^{-1} = \sigma^2(F) + 0.0013F^2$	$w^{-1} = \sigma^2(F) + 0.0006F^2$
no. of params	167	184	144
final R indices (obsd data) (%)	R = 2.66, R_w = 4.32	R = 2.79, R_w = 4.29	R = 2.56, R_w = 3.67
R indices (all data) (%)	R = 3.10, R_w = 4.78	R = 3.56, R_w = 4.74	R = 3.10, R_w = 3.92
goodness of fit	0.92	1.00	1.16
largest and mean Δ/σ	0.007, 0.001	0.003, 0.001	0.003, 0.000
data to param ratio	24.5:1	22.5:1	20.2:1
largest diff peak (e/Å^3)	0.54	0.71	0.55
largest diff hole (e/Å^3)	−0.38	−0.64	−0.43

[a] $F = F[1 + 0.002\chi F^2/(\sin 2\theta)]^{-1/4}$.

K) solution of 0.683 g of *trans*-$Ru(CO)_2(PEt_3)_2Cl_2$ (1) in 35 mL of THF. The temperature remained at 195 K for 2 h and then was gradually raised to 283 K. The crude reaction mixture was dried under vacuum and redissolved in CH_2Cl_2. One major band was collected by chromatography on silica gel under N_2 (eluant CH_2Cl_2/C_6H_{14} = 1:1). Solvent was removed on a rotavap and the product stored at 263 K. Crystallization from C_6H_{14} at 263 K gave 0.45 g of colorless crystals of **2** (52%). IR (CH_2Cl_2): ν(C≡C) 2021 m, ν(CO) 1986 s cm^{-1}. $^{31}P\{^1H\}$ NMR ($CDCl_3$): δ 19.9. $^{13}C\{^1H\}$ NMR ($CDCl_3$): δ 198.1 (t, CO, ^2J(P–C) = 13.4 Hz), 128.4 (t, C_α, ^2J(P–C) = 12.4 Hz), 116.1 (s, C_β), 18.6 (virtual triplet, CH_2), 7.7 (s, CH_3), 1.34 (s, $SiMe_3$). Anal. Calcd for $C_{24}H_{48}O_2P_2Si_2Ru$: C, 49.04; H, 8.23; P, 10.54. Found: C, 49.07; H, 8.12; P, 10.43.

Alternatively, compound **2** could be prepared from $SiMe_3C{\equiv}CSiMe_3$. A solution of LiMe/LiBr complex (1.4 mL) was added dropwise to 0.35 mL of $SiMe_3C{\equiv}CSiMe_3$ in 5 mL of THF at room temperature. After it was stirred for 3 h, the mixture was cooled to 195 K and added to the cold *trans*-$Ru(CO)_2(PEt_3)_2Cl_2$ (1; 0.33 g, 195 K) solution in 10 mL of THF. The reaction was complete after warming up to 293 K. Workup similar to that described above gave compound **2** in slightly lower yield.

***trans*-$Ru(CO)_2(PEt_3)_2(C{\equiv}CC{\equiv}CSiMe_3)_2$ (3).** After the addition of the LiMe/LiBr mixture (1.37 mL) to $SiMe_3C{\equiv}CC{\equiv}CSiMe_3$ (0.291 g in 5 mL of THF) at 195 K, the cooling bath was removed and the mixture was stirred at room temperature for 2 h. Both the $LiC{\equiv}CC{\equiv}CSiMe_3$ solution prepared in situ and *trans*-$Ru(CO)_2(PEt_3)_2Cl_2$ (1; 0.317 g in 10 mL THF) were cooled to 195 K prior to addition of one to the other via the use of a syringe. The reaction was carried out at 195 K for 2 h followed by slow warming to room temperature within the cooling bath. The dark brown crude mixture was dried under vacuum and the solution in CH_2Cl_2 separated by column chromatography (eluant CH_2Cl_2/C_6H_{14}, 2:8). The first band contained the product, which was very unstable in solution and slowly decomposed during the removal of solvent (as shown by a color change). Further separation upon TLC glass plates and crystallization from CH_2Cl_2/C_6H_{14} at 263 K gave 0.09 g of brown crystals of the product. IR (CH_2Cl_2): ν(C≡C) 2165 m, 2121 m; ν(CO) 2002 s cm^{-1}. $^{31}P\{^1H\}$ NMR ($CDCl_3$): δ 20.1. $^{13}C\{^1H\}$ NMR ($CDCl_3$): δ 196.4 (t, CO, $^2J_{P-C}$ = 12.8 Hz), 103.9 (t, C_2, $^2J_{P-C}$ = 12.5 Hz), 93.2, 92.4, 70.8 (3 singlets, C_3, C_4, and C_5), 18.9 (virtual triplet, CH_2), 7.6 (s, CH_3), 0.5 (s, $SiMe_3$). Proton-coupled ^{13}C NMR ($CDCl_3$): δ 196.3 (t, CO, $^2J_{P-C}$ = 13.0 Hz), 103.8 (t, C_2, $^2J_{P-C}$ = 13.5 Hz), 93.2, 92.3, 70.8 (3 singlets, C_3, C_4, and C_5), 18.8 (virtual triplet of triplets, CH_2, $^1J_{H-C}$ = 128.4 Hz), 7.6 (quartet, CH_3, $^1J_{H-C}$ = 128.1 Hz), 0.5 (quartet, $SiMe_3$, $^1J_{H-C}$ = 119.6 Hz). Anal. Calcd for $C_{28}H_{48}O_2P_2Si_2Ru$: C, 52.88; H, 7.60. Found: C, 53.00; H, 7.72.

***trans*-$Ru(CO)_2(PEt_3)_2(C{\equiv}CC{\equiv}CH)_2$ (4).** To *trans*-$Ru(CO)_2(PEt_3)_2(C{\equiv}CC{\equiv}CSiMe_3)_2$ (3) in 20 mL of THF, prepared as above but without further separation on TLC plates, was added 0.3 mL of Bu_4NF. The reaction was complete in 30 min as monitored by FTIR spectroscopy. The solvent was removed under vacuum, and the crude residue was dissolved in a minimum amount of CH_2Cl_2. Chromatography on silica gel (eluant CH_2Cl_2/C_7H_{16}, 1:1) and crystallization from CH_2Cl_2/C_6H_{14} at 263 K afforded light brown crystals of the desired product. Suitable crystals for X-ray analysis were obtained by further purification on TLC plates and recrystallization under the same conditions.

Table V. Atomic Coordinates (×10⁴) and Equivalent Isotropic Displacement Coefficients (Å² × 10⁴) for 2

	x	y	z	U(eq)[a]
Ru(1)	0	0	0	215.1 (7)
P(1)	1351.5 (3)	1689.6 (3)	541.2 (3)	258 (1)
Si(1)	3480.8 (4)	-2503.4 (4)	-371.9 (4)	335 (1)
O(1)	696 (1)	-704 (1)	2362.8 (9)	478 (5)
C(1)	458 (1)	-453 (1)	1490 (1)	299 (4)
C(2)	1379 (1)	-1041 (1)	-177 (1)	286 (4)
C(3)	2204 (1)	-1629 (2)	-295 (1)	367 (5)
C(4)	3588 (2)	-2284 (2)	-1715 (2)	527 (7)
C(5)	3272 (2)	-4157 (2)	-146 (2)	578 (8)
C(6)	4936 (2)	-1956 (2)	689 (2)	523 (7)
C(7)	1154 (2)	2608 (2)	1603 (1)	379 (5)
C(8)	1986 (2)	3727 (2)	1979 (2)	434 (6)
C(9)	2986 (1)	1335 (2)	1030 (1)	386 (5)
C(10)	3440 (2)	545 (2)	2042 (2)	508 (7)
C(11)	1217 (2)	2781 (2)	-525 (1)	400 (6)
C(12)	-3 (2)	3446 (2)	-962 (2)	538 (7)

[a] Equivalent isotropic U defined as one-third of the trace of the orthogonalized U_{ij} tensor.

IR (CH_2Cl_2): ν(C≡C) 2137 m, ν(CO) 2002 s, ν(≡CH) 3302 m cm^{-1}. ^1H NMR ($CDCl_3$): δ 2.0 (multiplet, 6 H, CH_2), 1.45 (t, 1 H, ≡CH, $^6J_{P-H}$ = 0.8 Hz), 1.19 (multiplet, 9 H, CH_3). $^{31}P\{^1H\}$ NMR ($CDCl_3$): δ 20.0. $^{13}C\{^1H\}$ NMR ($CDCl_3$): δ 196.3 (t, CO, $^2J_{P-C}$ = 12.2 Hz), 101.3 (t, C_2, $^2J_{P-C}$ = 12.0 Hz), 91.7 (s, C_3), 72.1 (s, C_4), 54.5 (s, C_5), 18.8 (virtual triplet, CH_2), 7.6 (s, CH_3). Proton-coupled ^{13}C NMR ($CDCl_3$): δ 196.4 (t, CO, $^2J_{P-C}$ = 12.4 Hz), 101.3 (t, C_2, $^2J_{P-C}$ = 13.7 Hz), 91.7 (s, C_3), 72.1 (d, C_4, $^2J_{H-C}$ = 50.8 Hz), 54.5 (d, C_5, $^1J_{H-C}$ = 252.0 Hz), 18.8 (virtual triplet of triplets, CH_2, $^1J_{H-C}$ = 127.8 Hz), 7.6 (quartet, CH_3, $^1J_{H-C}$ = 127.8 Hz).

***trans*-Ru(CO)$_2$(PEt$_3$)$_2$(C≡CH)$_2$ (5).** A dry, three-necked 100-mL flask equipped with a magnetic stirring bar and septum-capped inlet was flushed with nitrogen. Diethyl ether (30 mL) was placed in the flask, and the flask was cooled to 195 K. The solvent was then saturated with HC≡CH gas (dried by concentrated H_2SO_4(l), KOH(s), and $CaCl_2$(s) in that order). The gas was bubbled rapidly through the solution for an extra 15 min and the bubbling continued during the slow addition of Bu^{n}Li (2 mL). One hour later, the HC≡CH inlet was switched to a nitrogen flow and cold *trans*-Ru(CO)$_2$(PEt$_3$)$_2$Cl$_2$ (1; 0.6 g in 10 mL of THF, 195 K) was transferred through a syringe to the lithium acetylide solution. The mixture was then warmed up slowly to room temperature, and the stirring was continued at this temperature for 5 h. The solvent was removed under vacuum, and the dark brown mixture was separated by chromatography on silica gel (eluant CH_2Cl_2/C_6H_{14}, 2:1). The acetylide was isolated in the major band. Crystals of 5 (0.21 g) were collected after crystallization from hexane at 263 K (yield 34%). IR (CH_2Cl_2): ν(C≡C) 1944 m, ν(CO) 1987 s, ν(≡CH) 3271 m cm^{-1}. ^1H NMR ($CDCl_3$): δ 2.05 (multiplet, 6 H, CH_2), 1.54 (t, 1 H, ≡CH, $^4J_{P-H}$ = 1.7 Hz), 1.19 (multiplet, 9 H, CH_3). $^{31}P\{^1H\}$ NMR ($CDCl_3$): δ 19.9. $^{13}C\{^1H\}$ NMR ($CDCl_3$): δ 198.4 (t, CO, $^2J_{P-C}$ = 13.4 Hz), 98.5 (t, C_α, $^2J_{P-C}$ = 13.0 Hz), 95.0 (s, C_β), 18.6 (virtual triplet, CH_2), 7.7 (s, CH_3). Proton-coupled ^{13}C NMR ($CDCl_3$): δ 196.4 (t, CO, $^2J_{P-C}$ = 13.3 Hz), 98.5 (multiplet, C_α), 95.1 (d, C_β, $^1J_{H-C}$ = 222.7 Hz), 18.5 (virtual triplet of triplets, CH_2, $^1J_{H-C}$ = 129.1 Hz), 7.6 (quartet, CH_3, $^2J_{H-C}$ = 127.6 Hz). Anal. Calcd for $C_{18}H_{32}O_2P_2Ru$: C, 48.75; H, 7.27; P, 13.97. Found: C, 48.50; H, 7.18; P, 14.12.

Crystallography. The X-ray studies were carried out with a Siemens R3m/v automated diffractometer. Intensity data were obtained with graphite-monochromated Mo Kα radiation (λ = 0.710 73 Å) at 200 K by employing the ω-scan technique with a 2θ range from 4.0 to 60.0°. Two standard reflections were monitored every 100 measurements. No significant decay was noticed during any of the data collections. Intensities were corrected for Lorentz and polarization effects. The structures were solved by Patterson and Fourier methods and refined by full-matrix least squares, with use of the Siemens SHELXTL PLUS software. All non-hydrogen atoms were refined anisotropically, while the hydrogen atoms were refined with isotropic thermal parameters in their calculated position. A face-indexed numerical method was applied to correct for absorption effects. Cell constants and data collection and final refinement details are given in Table IV. Atomic coordinates and equivalent isotropic displacement coefficients are listed in Tables V–VII.

Table VI. Atomic Coordinates (×10⁴) and Equivalent Isotropic Displacement Coefficients (Å² × 10³) for 3

	x	y	z	U(eq)[a]
Ru(1)	0	0	0	24.53 (7)
P(1)	1322.5 (3)	801.0 (4)	-516.2 (3)	30.0 (1)
Si(1)	4125.6 (4)	-964.1 (5)	6091.2 (4)	33.6 (2)
O(1)	650 (1)	-2769 (2)	-266 (2)	60.8 (8)
C(1)	396 (1)	-1747 (2)	-195 (2)	37.1 (6)
C(2)	1104 (1)	-137 (2)	1644 (2)	31.7 (6)
C(3)	1757 (2)	-292 (2)	2617 (2)	35.7 (6)
C(4)	2481 (1)	-488 (2)	3704 (2)	35.3 (6)
C(5)	3120 (1)	-658 (2)	4664 (2)	39.0 (6)
C(6)	4873 (2)	567 (3)	6669 (2)	52.4 (8)
C(7)	3469 (2)	-1518 (3)	6986 (2)	50.4 (8)
C(8)	5064 (2)	-2186 (3)	6014 (2)	62 (1)
C(9)	1037 (2)	682 (3)	-1995 (2)	62 (1)
C(10)	922 (3)	-711 (5)	-2447 (3)	97 (2)
C(11)	2599 (2)	26 (2)	213 (2)	47.5 (9)
C(12)	3500 (2)	571 (3)	-36 (2)	62 (1)
C(13)	1604 (2)	2526 (2)	-253 (2)	53 (1)
C(14)	2089 (3)	2887 (3)	976 (3)	79 (2)

[a] Equivalent isotropic U defined as one-third of the trace of the orthogonalized U_{ij} tensor.

Table VII. Atomic Coordiantes (×10⁴) and Equivalent Isotropic Displacement Coefficients (Å² × 10⁴) for 4

	x	y	z	U(eq)[a]
Ru(1)	0	0	0	186.0 (6)
P(1)	976.7 (5)	1795.5 (4)	963.9 (2)	204 (1)
O(1)	3268 (2)	411 (2)	-977.2 (9)	384 (4)
C(1)	2056 (2)	286 (2)	-626 (1)	250 (4)
C(2)	-1430 (2)	1532 (2)	-687 (1)	247 (4)
C(3)	-2262 (2)	2379 (2)	-1100 (1)	287 (5)
C(4)	-3180 (2)	3335 (2)	-1616 (1)	306 (5)
C(5)	-3948 (3)	4162 (3)	-2068 (1)	406 (6)
C(6)	-255 (2)	3506 (2)	972 (1)	267 (4)
C(7)	-2122 (2)	3340 (2)	1242 (1)	339 (5)
C(8)	3228 (2)	2398 (2)	837 (1)	277 (5)
C(9)	3377 (3)	3447 (2)	120 (1)	356 (5)
C(10)	981 (2)	1126 (2)	2010 (1)	282 (5)
C(11)	1540 (3)	2210 (2)	2675 (1)	341 (5)

[a] Equivalent isotropic U defined as one-third of the trace of the orthogonalized U_{ij} tensor.

Acknowledgment. We are very grateful to the Natural Sciences and Engineering Research Council of Canada for financial support of this work in the form of a Strategic Group Grant.

Supplementary Material Available: Tables giving structure determination summaries, anisotropic thermal parameters, and hydrogen atom positional and thermal parameters for 2–4 (15 pages). Ordering information is given on any current masthead page. Tables of observed and calculated structure factors (2, 17 pages; 3, 19 pages; 4, 13 pages) are available upon request from the authors.

OM920272D